Published in final edited form as:
Science. 2007 October 12; 318(5848): 279–283. doi:10.1126/science.1146113.

Fluorescence-force spectroscopy maps two-dimensional reaction landscape of the Holliday junction

Sungchul Hohng[1,2,†], **Ruobo Zhou**[1], **Michelle K. Nahas**[1], **Jin Yu**[1,4], **Klaus Schulten**[1,4], **David M. J. Lilley**[5], and **Taekjip Ha**[1,2,3,4,*]

[1]Department of Physics, University of Illinois at Urbana-Champaign, Urbana, Illinois 61801, USA

[2]Howard Hughes Medical Institute, Urbana, Illinois 61801 USA

[3]Center for Biophysics and Computational Biology, University of Illinois at Urbana-Champaign, Urbana, Illinois 61801, USA

[4]Beckman Institute, University of Illinois at Urbana-Champaign, Urbana, Illinois 61801, USA

[5]Cancer Research UK Nucleic Acid Structure Research Group, Department of Biochemistry, MSI/WTB complex, The University of Dundee, Dundee DD1 5EH, U.K.

Abstract

Despite the recent advances in single molecule manipulation techniques, purely mechanical approaches can not detect subtle conformational changes in the biologically important regime of weak forces. We developed a hybrid scheme combining force and fluorescence which allowed us to examine the effect of sub-pN forces on the nanometer scale motion of the Holliday junction (HJ) at 100 Hz bandwidth. The HJ is an exquisitely sensitive force sensor whose force response is amplified with an increase in its arm lengths, demonstrating a lever-arm effect at the nanometer length scale. Mechanical interrogation of the HJ in three different directions helped elucidate the structures of the transient species populated during its conformational changes. This method of mapping two dimensional reaction landscapes at low forces is readily applicable to other nucleic acid systems and their interactions with proteins and enzymes.

Many biological processes are dependent on tension. In recent years, single molecule force measurements have shown directly that biochemical reactions can be influenced by applied force (1). Yet, purely mechanical tools can not detect small scale conformational changes unless strong enough and persistent force is applied. At weak forces, the flexible tether connecting the mechanical probe to the biological molecule is not stretched enough to transmit small movements. This is unfortunate because weak and transient forces are likely more prevalent *in vivo* but the experimental limitations confine single molecule mechanical studies to examining the effect of relatively large forces. We aimed to study the effect of weak external forces on the biomolecular conformational dynamics by combining single molecule fluorescence resonance energy transfer (smFRET) (2–4) with manipulation using optical trap (5). smFRET has high spatial resolution (≤ 5 Å) (6, 7)) and can be measured at arbitrarily low forces. Previous attempts to combine FRET and optical trap using the DNA hairpin as a model system (8, 9) did not reveal new information because the hairpin unzips at high forces (~ 15 pico Newton (pN)), a regime that had been extensively investigated using force-based techniques (10, 11). Here, we report an approach to detect nanometer-

*To whom correspondence should be addressed. (tjha@uiuc.edu).
†Present Address: Department of Physics and Astronomy, Seoul National University, Seoul 151-742, Korea.

scale motion at sub-pN forces. We used the approach to gain insight into the reaction landscape of the Holliday junction (HJ) by gently stretching it along different directions.

The HJ is a four-stranded DNA structure that forms as an intermediate during recombination (12). To understand the mechanisms of cellular enzymes that function with the HJ, a detailed description of the static and dynamic structural properties of the HJ itself is needed. In the absence of added ions the HJ adopts an open structure, where the four helical arms point toward the corners of a square (13, 14) (Fig. 1A). In the presence of physiological concentrations of magnesium ions, the HJ becomes more compact by pairwise coaxial stacking of helical arms into a right-handed antiparallel stacked-X structure(13–15). There are two ways of forming this stacked structure that depend upon the choice of helical stacking partners (*iso*I and *iso*II) (Fig. 1B). For these studies, we have chosen a sequence with nearly equal population of stacking conformers *iso*I and *iso*II (16) (17) (Fig. S1). smFRET studies showed that a HJ continually switches between the two stacking conformations (18). At present, there is no structural information on the transient species populated during these conformational changes.

To investigate the nature of such transient HJ structures and to understand how HJ conformational properties could depend on physiologically relevant forces, we built a hybrid instrument that combines smFRET with optical trapping via a long linker (bacteriophage λ DNA)(17). The trapping and fluorescence excitation beams in our confocal microscope are spatially separated (minimum 13 μm, Fig. 1C) such that fluorescence and force processes can operate without mutual interference. The long linker acts as a loose spring that dampens the random forces generated by Brownian motion of the trapped bead and reduces force variations due to the nanometer-scale conformational change of the HJ. The effective stiffness of the λ DNA at 2 pN of force is about 0.002 pN/nm such that 5 nm movement of the HJ causes negligible force fluctuations (~0.01 pN) at the trapped bead. Therefore, the measurements can be performed under effectively constant force without the need for active force clamping. The relaxation time scales of the λ DNA under tension are faster than the time scale of conformational fluctuations we investigate here(19). The trapping beam (1,064 nm) was fixed along the optical axis of the microscope, and force was applied by moving the surface-tethered HJ using a piezoelectric sample scanner. The confocal excitation beam (532 nm) was programmed to follow the HJ using a piezo-controlled mirror to maintain uniform excitation and detection efficiencies regardless of the specimen location (and therefore force) (17)

To determine comprehensively the force response of the HJ, we used the following four constructs (Fig. 1A). The four helices comprising the HJ are named B (red), H (green), R (dark gray), and X (gray). Helix R was labeled at its 5’ terminus with biotin for surface immobilization, and helices X, H, or B were extended by a 12 nt ssDNA 5’-overhang to permit annealign to a cohesive end of λ-DNA (named junctions *XR, HR* and *BR* respectively). The other end of the λ-DNA was attached to a bead via digoxigenin/anti-digoxigenin coupling in order to pull on the DNA using optical tweezers in three different directions, between X and R arms for junction *XR* etc. Junctions *XR* and *XR*-long differ in the length of the X and R arms (11 bp vs. 21 bp). Cy3 (FRET donor), was attached to the 5’-terminus of helix H, and Cy5 (acceptor) to the 5’-end of helix B. For junctions *XR* and *XR*-long, the stretching force should favor *iso*I (low FRET), in which there is a larger separation between the two tether points, over *iso*II (high FRET) (Fig. 1D). Indeed, single molecule FRET histograms as a function of force show that the low FRET state is significantly favored at forces exceeding 0.5 and 1.0 pN for junctions *XR*-long and *XR* respectively (Fig. 1E and 1F). Likewise, *iso*II (high FRET) would be favored at high forces for junction *HR*. In contrast, the two tether points would have similar distances for *iso*I and *iso*II in the case of junction *BR*and force-induced bias should be minimal.

Fig. 2A shows smFRET time traces at five different forces (gray lines, 10 s duration each with 10 ms integration time) obtained from a single molecule of junction *XR*. Enhanced photostability by means of the use of Trolox (20) allowed us to obtain one to five cycles of force data from a single molecule before photobleaching, corresponding to observation over 50 to 250 s. Idealized FRET trajectories generated by hidden Markov modeling (red lines) (21) are also shown. At the lowest force (0.3 pN), the junction switches between the high and low FRET states with similar populations. As the force exceeds 1 pN, the dynamics become clearly biased to the low FRET state. Fig. 2B shows the transition rates determined from hidden Markov modeling as a function of force. The transition rate k_f for the forward reaction from the low FRET state (*iso*I) to the high FRET state (*iso*II) decreases with increasing force (blue), while the transition rate for the backward reaction k_b (*iso*II to *iso*I) increases with force (red) as expected. Both changes were linear in the log-linear scale but interestingly, k_f had twice the slope of k_b. If the reaction is viewed as possessing a single transition state, the slope reflects the distance to the transition state (1). Therefore, the transition state lies closer to *iso*II than to *iso*I when force is applied via the *XR* vector. Averaged over five molecules, the distance from *iso*II to the transition state ($\Delta x_b^{\ddagger}$) is 1.5 ± 0.3 nm and the distance from *iso*I to the transition state ($\Delta x_f^{\ddagger}$) is 2.9 ± 0.6 nm (Table 1).

We next studied junction *HR* where the λ DNA tether has been transferred from the X to the H arm. In this construct, the force is expected to bias the HJ to the high FRET *iso*II state, and indeed this was the result (Fig. 2C). k_b decreased and k_f increased with stronger forces, but with two-fold higher slope for k_b than for k_f (Fig. 2D). Averaged over five molecules, $\Delta x_b^{\ddagger}$=2.4 ± 0.5 nm and $\Delta x_f^{\ddagger}$=1.3 ± 0.3 nm. In both junctions, ($\Delta x_b^{\ddagger}$+$\Delta x_f^{\ddagger}$) is equal to the distance between *iso*I and *iso*II, Δx_{eq}calculated from equilibrium population vs. force data (Table I). Therefore, the distances between the ends of the pulled arms, d_{XR} for junction *XR* and d_{HR} for junction *HR*are suitable reaction coordinates spanning the complete trajectory from *iso*I to *iso*II (Fig. 3A).

In one pulling direction represented by $d_{XR}$the transition state lies closer to *iso*II (Fig. 3A, middle panel) while for the other pulling direction along $d_{HR}$the transition state more closely resembles *iso*I (Fig. 3A, bottom panel). These two transition states can not represent a single structure because then both d_{XR} and d_{HR} must be relatively small, and by symmetry so must be d_{XB} and d_{HB}. Such a structure would have all four helices in the same hemisphere relative to the junction core which is highly unlikely considering the symmetry of the HJ. Instead, we favor a model where there are at least two different transition states, *ts*I and *ts*II, equal in energy but corresponding to different values of d_{XR} (or d_{HR}), such that force would elevate one of them into the single highest energy barrier via the tilting of the energy landscape (Fig. 3A).

The data presented so far show that the distance change upon stacking conformer transitions is about 4 nm. Since thermal energy is about 4 pN-nm, a force on the order of 1 pN would consequently change the equilibrium between the two states by 2–3 fold. Such small scale conformational fluctuations at these low forces are probably impossible to detect in a purely mechanical measurement, especially at our time resolution (10 ms).

What determines the force sensitivity of the junction? Is it an intrinsic property of the junction core or is it dependent on the length of helical arms on which the force is applied? Since the four arms of the HJ meet at its center, we may recast the experimental configuration as a torque being applied around the central pivot point. The torque is proportional to the product of the magnitude of force and the distance between the point of application of the force and the pivot point (i.e., the length of the arm). Therefore, it could be expected that increasing arm length would result in a greater torque for the same force. We tested such a lever arm effect using junction *XR*-long, where the X and R arms are

lengthened by about a factor of two (from 11 bp to 21 bp) compared to junction *XR*. FRET histograms as a function of applied force (Fig. 1E and Fig. 1F) show that increasing the lever arm length has magnified the force effect such that much lower force is needed for junction *XR*-long to achieve the same conformational bias. Fig. S4 compares the transition rates vs. force between five molecules each of junctions *XR* and *XR*-long each and shows that junction XR-long exhibits much greater changes in rates for the same magnitude of force (also compare $\Delta x_f^{\ddagger}$ and $\Delta x_b^{\ddagger}$ in Table I). Since the persistence length of double stranded DNA is about 50 nm (~ 150 bp) (22) the lever arm effect can probably be extended by another factor of five for arms of ≥ 100 bp. That is, forces as low as 0.1 pN would be enough to influence the junction conformations, illustrating the exquisite force sensitivity of the HJ.

Since the effect of force depends on the arm lengths, the most natural reaction coordinates are angular. The angles that define the global shape of the junction are ϕ, the interhelical angle between two stacked pairs of helices, and ψ, the angle that measures the degree of unstacking of stacked helices (23) (Fig. 3B). For example, for a stacked-X structure ϕ=40° and ψ=0° (15), while for an open structure, ϕ is 0° and ψ is 90° (Fig. 3C). These two angles are well-defined within the angular space in which identities of stacking pairs are maintained. Our aim here is to deduce the structure of the transition state by determining the ϕ and ψ values of the transition state using a geometrical analysis. The analysis below estimates the angles ($\phi_{II}\psi_{II}$) of the transition state *ts*II in the *iso*II half of the conformational reaction coordinate, but the same conclusions hold for *ts*I.

*ts*II lies a third of the way from *iso*II to *iso*I along the d_{XR} coordinate (Table 1, Fig. 3A). We can show that this condition is satisfied for a collection of ($\phi_{II}\psi_{II}$) values, starting from (70°, 0°) at one extreme and arriving at (0°, 70°) at the other (Fig. 3C, gray zone) (18). In order to obtain an additional constraint, we performed an equivalent force analysis on junction *BR* (Fig. 2E, 2F, Table 1). Junction *BR* exhibited much reduced (by 5–6 fold) force dependence of the equilibrium populations compared to junctions *XR* and *HR* (compare Δx_{eq} values in Table 1). The residual force dependence of the equilibrium populations may be attributed to the finite diameter of the DNA duplex (18). In contrast to junctions *XR* and *HR*application of force on junction *BR* accelerated both forward and backward transitions (Fig. 2F). Therefore, the distance between the ends of B and R arms, d_{BR}, must be larger in the transition state than in the stacked-X structures. This condition is satified only if ϕ_{II} in the transition state is smaller than the 40° of the stacked-X structure. Furthermore, the distance to the transition state is 0.37 nm at minimum which constrains ϕ_{II} to be essentially zero (18). In combination, our best estimate is $(\phi_{II}\psi_{II})_{ts}$= (0°, 70°) for *ts*II (Fig. 3C). This transition state is similar to the open state, but with arms deviating by about 20° from the ideal open state while displaying signatures on which pairs of helices are nearly stacked over each other (Fig. 3D). The structure bears a strong resemblance to the HJ structure bound to the Cre recombinase (24). Following the same argument, we can deduce that the transition state in the *iso*I-like conformational space, *ts*I, also has $(\phi_I\psi_I)_{ts}$= (0°, 70°).

By probing the HJ dynamics in response to pulling forces in three different directions, we mapped the location of the transition states in the two-dimensional reaction landscape and deduced the global structure of the transient species populated during the HJ conformational changes. Our simplest model envisions a shallow minimum between the two transition states, depicted as the open structure (Fig. 3A and 3D), but it is also possible that a continuum of conformations exist, spanning from *ts*I and *ts*II with nearly identical free energies, instead of having a single well-defined minimum.

The development reported here expands on the current arsenal of hybrid single molecule techniques combining force and other observables (8, 25–27). Unlike DNA or RNA

hairpins, where forces on the order of 15 pN are necessary to induce mechanical unzipping (10, 11), the conformations of HJs could be biased at 0.5 pN or lower. The lever arm effect makes it unlikely that a purely mechanical tool could have probed the force effect on HJ conformations because if the arms are lengthened to magnify the distance change, the force effect will occur at even lower forces. FRET can also report on vectors other than the end-to-end distances which we exploited here by pulling on *XR, HR* or *BR* arms while simultaneously measuring the same HB vector via FRET, which led to the two dimensional mapping of reaction landscapes. Our method is readily applicable to other nucleic acids systems and their interaction with proteins and enzymes, and with the advent of new orthogonal labeling techniques, should be extendable to proteins and protein complexes. The next technical challenge would be to obtain time evolution of the end-to-end distance by force, for example due to the action of DNA processing enzymes (28), and correlate it with the enzyme conformational changes simultaneously measured via fluorescence.

Supplementary Material

Refer to Web version on PubMed Central for supplementary material.

Acknowledgments

We thank Wei Cheng at UC Berkeley for providing the protocol for the preparation of anti-Dig coated bead, Michelle Wang at Cornell University for giving generous advices about building optical tweezers, Yann Chemla at University of Illinois for helpful discussion, and Chirlmin Joo for generous help in preparation of illustrations. Funding was provided by the National Sciences Foundation CAREER Award (PHY 0134916) and the National Institutes of Health (GM065367).T.H. is an investigator with the Howard Hughes Medical Institute.

References and notes

1. Bustamante C, Chemla YR, Forde NR, Izhaky D. Annu Rev Biochem. 2004; 73:705. [PubMed: 15189157]
2. Stryer L, Haugland RP. Proc. Natl. Acad. Sci., USA. 1967; 58:719. [PubMed: 5233469]
3. Ha T, et al. Proceedings of the National Academy of Sciences of the United States of America. 1996; 93:6264. [PubMed: 8692803]
4. Ha T. Methods. 2001; 25:78. [PubMed: 11558999]
5. Ashkin A, Dziedzic JM, Bjorkholm JE, Chu S. Optics Letters. 1986; 11:288. [PubMed: 19730608]
6. Kapanidis AN, et al. Science. 2006 Nov 17.314:1144. [PubMed: 17110578]
7. Blanchard SC, Gonzalez RL, Kim HD, Chu S, Puglisi JD. Nat Struct Mol Biol. 2004 Oct.11:1008. [PubMed: 15448679]
8. Lang MJ, Fordyce PM, Block SM. Journal of Biology. 2003; 2:6. [PubMed: 12733997]
9. Tarsa PB, et al. Angew Chem Int Ed Engl. 2007; 46:1999. [PubMed: 17279589]
10. Liphardt J, Onoa B, Smith SB, Tinoco I, Bustamante C. Science. 2001; 292:733. [PubMed: 11326101]
11. Woodside MT, et al. Science. 2006 Nov 10.314:1001. [PubMed: 17095702]
12. Holliday R. Genet. Res. 1964; 5:282.
13. Duckett DR, et al. Cell. 1988; 55:79. [PubMed: 3167979]
14. Lilley DMJ. Quarterly Reviews of Biophysics. 2000; 33:109. [PubMed: 11131562]
15. Eichman BF, Vargason JM, Mooers BHM, Ho PS. Proceedings of the National Academy of Sciences of the United States of America. 2000; 97:3971. [PubMed: 10760268]
16. Grainger RJ, Murchie AIH, Lilley DMJ. Biochemistry. 1998; 37:23. [PubMed: 9425022]
17. Materials and methods are available as supporting material on Science Online.
18. McKinney SA, Declais AC, Lilley DMJ, Ha T. Nature Structural Biology. 2003; 10:93.
19. Meiners JC, Quake SR. Physical Review Letters. 2000; 84:5014. [PubMed: 10990855]
20. Rasnik I, McKinney SA, Ha T. Nat Methods. 2006 Nov.3:891. [PubMed: 17013382]

21. McKinney SA, Joo C, Ha T. Biophys J. 2006 Sep.91:1941. [PubMed: 16766620]
22. Bustamante C, Marko JF, Siggia ED, Smith S. Science. 1994; 265:1599. [PubMed: 8079175]
23. Yu J, Ha T, Schulten K. Nucleic Acids Res. 2004; 32:6683. [PubMed: 15613597]
24. Van Duyne GD. Annu Rev Biophys Biomol Struct. 2001; 30:87. [PubMed: 11340053]
25. Ishijima A, et al. Cell. 1998; 92:161. [PubMed: 9458041]
26. Shroff H, et al. Nano Lett. 2005 Jul.5:1509. [PubMed: 16178266]
27. Gore J, et al. Nature. 2006 Jan 5.439:100. [PubMed: 16397501]
28. Lee JB, et al. Nature. 2006 Feb 2.439:621. [PubMed: 16452983]

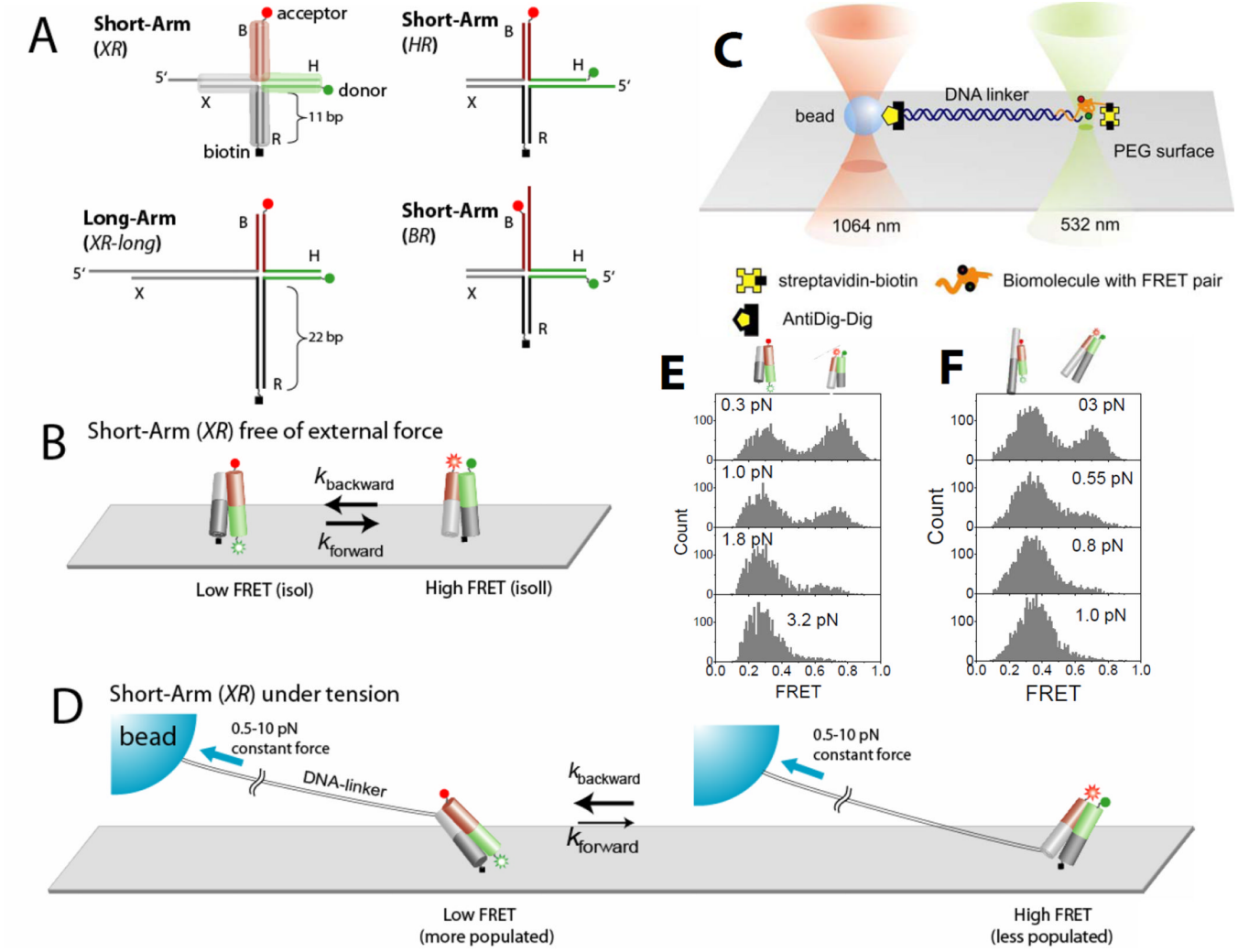

Fig. 1.

Holliday junction constructs and experimental scheme. (A) The HJ species studied. Junction *XR* comprises four arms of 11 bp, termed B (red), H (green), R (dark gray) and X (gray). Cy3 and Cy5 fluorophores are terminally attached to H and B arms respectively, and the molecule is tethered to the surface through biotin attached to the end of the R arm. Stretching force is applied through the λ-DNA linker hybridized to the X arm. In junction *XR*-long the lengths of arms R and X are increased to 21 bp. In junction *HR* the λ-DNA linker is hybridized to the H arm. In junctions *HR* and *BR* the λ-DNA linker is hybridized to the H and B arms respectively. (B) Junction *XR* is known to alternate between two different stacking conformers, *iso*I (Low FRET) and *iso*II (High FRET) with similar populations in both states. (C) A surface-immobilized biomolecule with FRET labeling is connected to a trapped bead via a long DNA linker. The linker DNA spatially separates the confocal beam (532 nm) from the trapping beam (1064 nm) such that enhanced photobleaching and an overwhelming background signal induced by the intense trapping laser are avoided. To apply force, the surface immobilized molecule was moved relative to the trapped bead. The confocal beam was programmed to follow the motion of the molecule using the mapping generated between sample scanning and beam scanning (Fig. S6). (D) Force is expected to bias the junction *XR* to *iso*I which possesses a larger separation between the two tether

points than *iso*II. (E) FRET histograms of a single junction *XR* as a function of force. (F) FRET histograms of a single junction *XR*-long as a function of force.

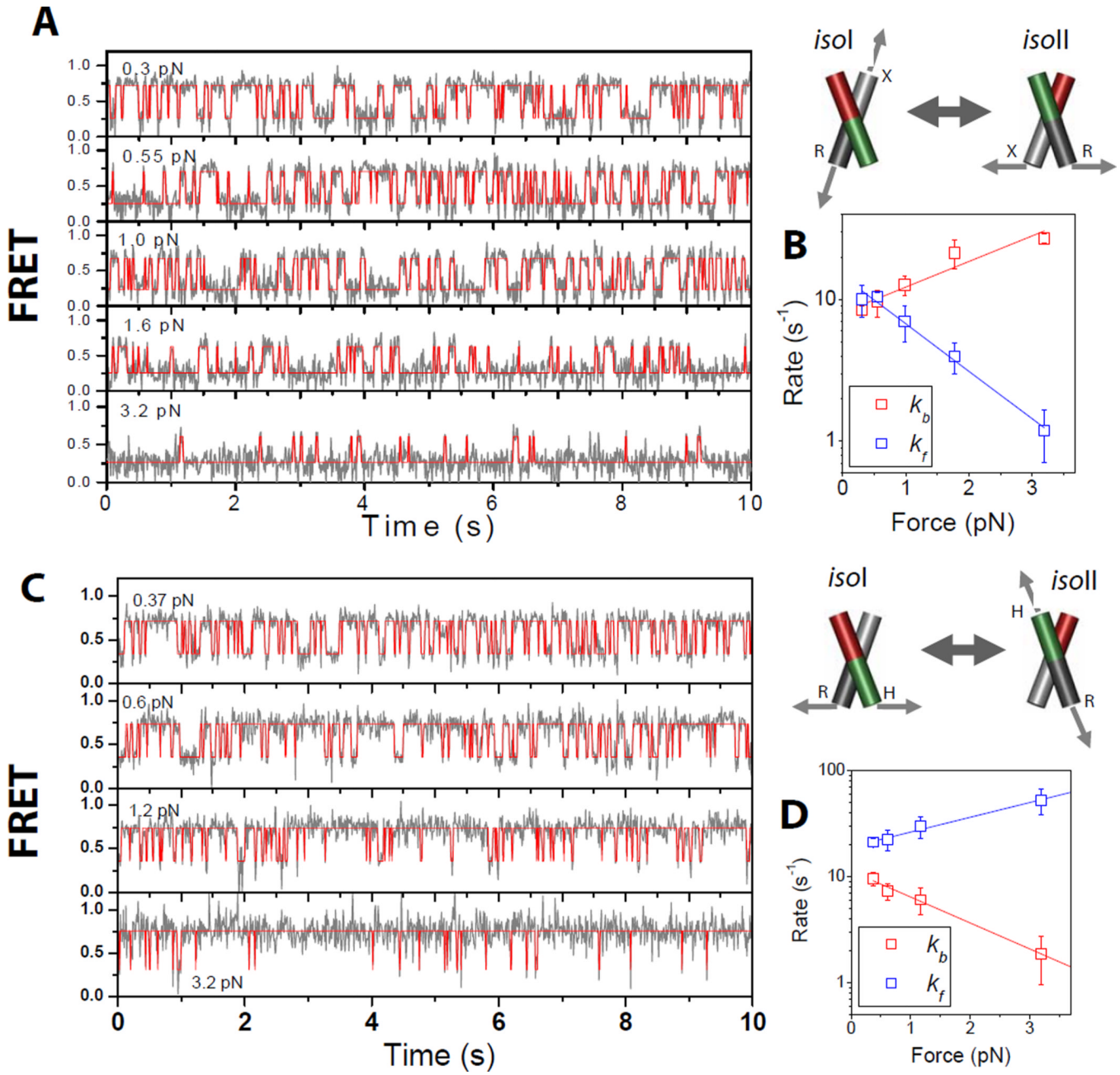

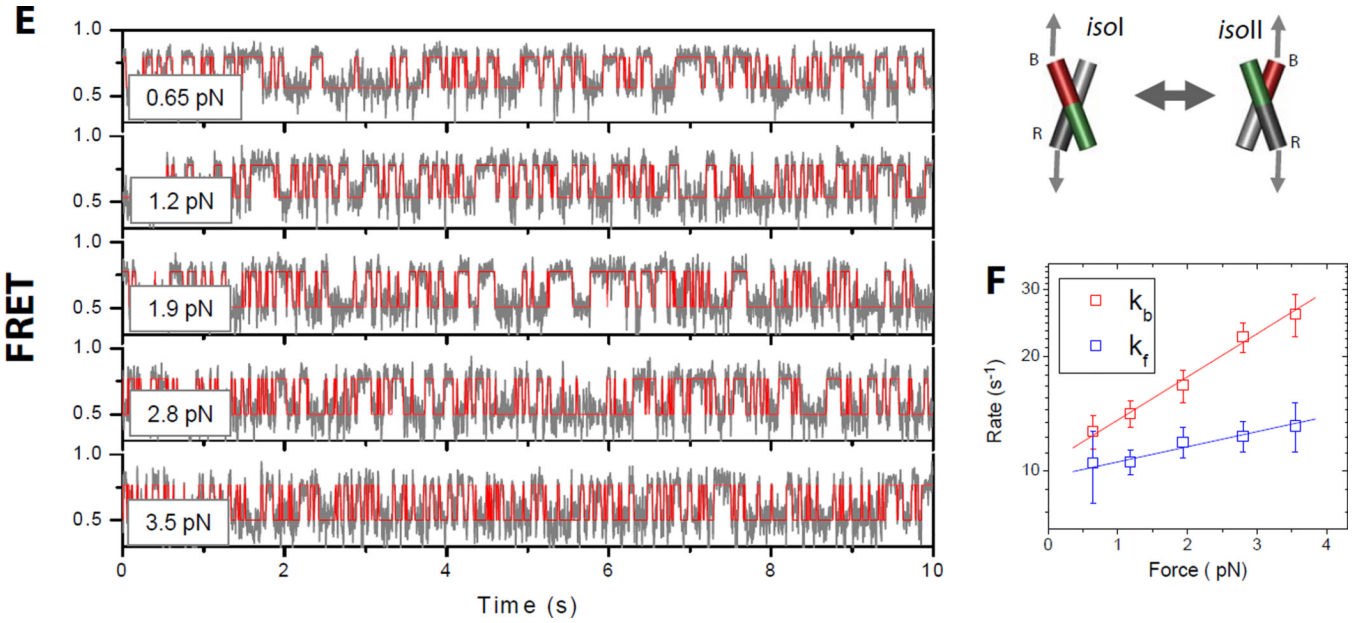

Figure 2.

Conformer exchange dynamics of the HJ as a function of applied force. (A) FRET time traces (gray lines) of a single junction *XR* molecule at different forces. FRET efficiency is approximated by the acceptor intensity divided by the sum of the donor and acceptor intensities. Red lines are the most likely FRET trajectories generated via hidden Markov modeling. The imposed force (indicated on the top left of each plot) increases top to bottom. (B) Log-linear plot of rate constants of conformer exchange as a function of force. Rates of transitions from states *iso*II to *iso*I (k_b red) and *iso*I to *iso*II (k_f blue) are differentiated by color. Error bars represent standard deviations obtained from repeated measurements of the same molecule. From linear fitting, we found that the transition state is closer to *iso*II (1.8 nm) than to *iso*I (3.3 nm). (C) Same as (A) but for a single junction *HR* molecule. (D) Same as (B) for a single junction *HR* molecule. (E) Same as (A) and (C) but for a single junction *BR* molecule. (F) Same as (B) and (D) but for a single junction *BR* molecule.

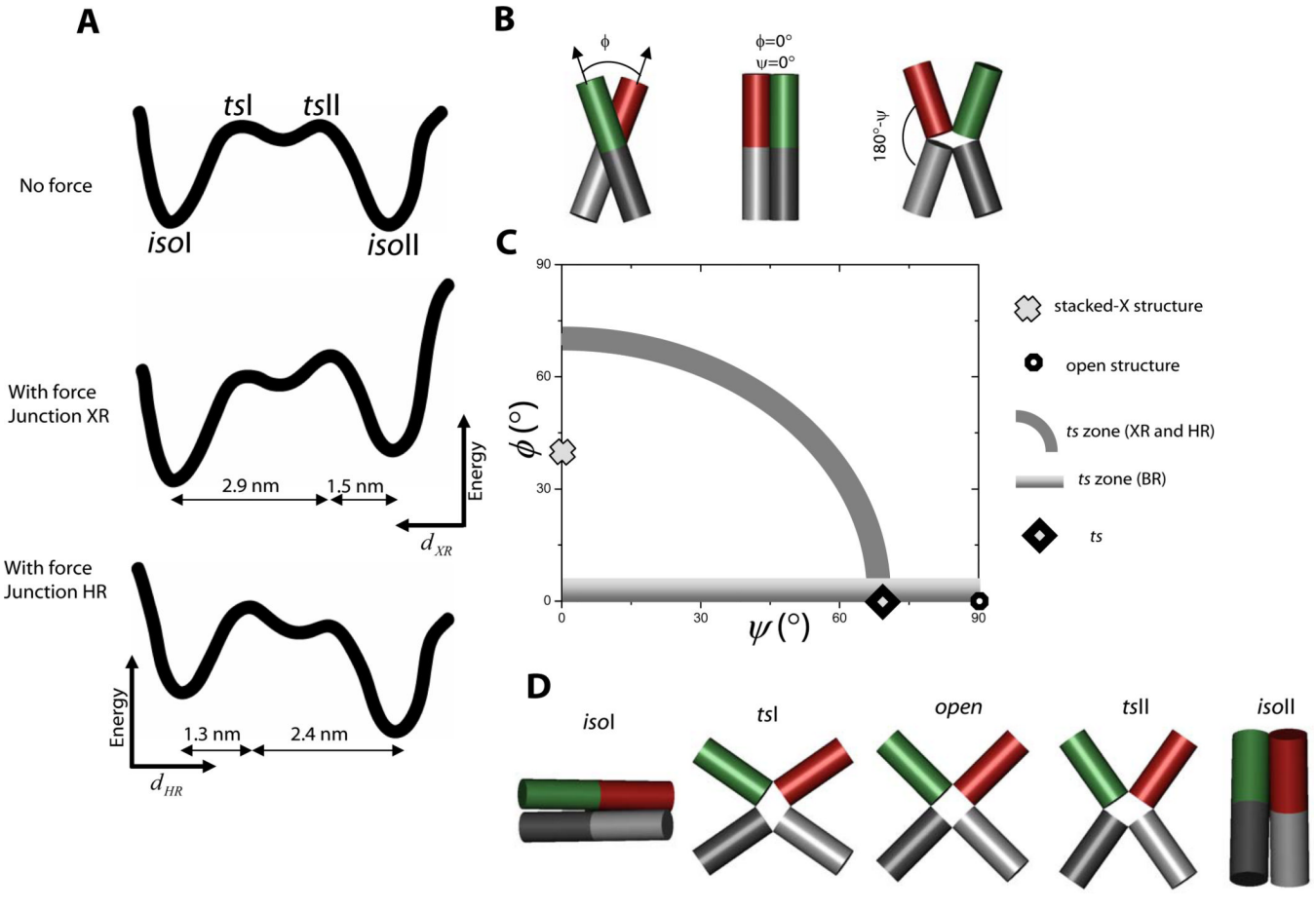

Figure 3.

Mapping the reaction landscape and determining the transition state structure. (A) A proposed reaction landscape with two distinct transition states with nearly identical energies (top). In junction *XR* the applied force would tilt the energy landscape toward *isoI* so that the transition state, *ts*II, nearer to *iso*II would become the state of highest energy along the entire coordinate (middle). The reaction coordinate here is the distance between the ends of X and R arms, d_{XR} which increases to the left as shown. Similarly, in junction *XR* the transition state, *ts*I, nearer to *iso*I would become the single transition state upon application of force. The reaction coordinate here is the distance between the ends of H and R arms, d_{HR} which increases to the right. (B) Two angular coordinates ϕ and ψ define the global conformation of the HJ. (C) Two-dimensional conformational space of HJ conformations. The stacked-X structure and open structure are marked. The gray arc represents a zone that satisfies experimental constraints derived from *XR* and *HR* data, and the gradient zone is derived from *BR* data. The consensus location of the transition state is marked with a diamond. (D) Global structures of *iso*I, *iso*II and two transition states, *ts*I and *ts*II, plus an open structure.

Table 1

Distance to the transition state from *iso*I ($\Delta x_f^{\ddagger}$) and from *iso*II ($\Delta x_b^{\ddagger}$) measured from the force-dependent transition rates between *iso*I and *iso*II for four different junctions. Errors represent standard deviation from five different molecules each. Also shown is Δx_{eq}, the distance between *iso*I and *iso*II determined from force-dependent changes in the equilibrium constant. For junction *BR*, Δx_{eq} deviates significantly from ($\Delta x_b^{\ddagger}+\Delta x_f^{\ddagger}$) showing that d_{BR} is not a valid reaction coordinate connecting *iso*I and *iso*II. In contrast, $\Delta x_{eq}=\Delta x_b^{\ddagger}+\Delta x_f^{\ddagger}$ within error for junctions *XR* and *HR* showing that d_{XR} and d_{HR} are reaction coordinates valid from *iso*I to *iso*II.

	XR	XR-long	HR	BR
$\Delta x_b^{\ddagger}$ (nm)	1.5 (±0.3)	2.6 (±0.6)	2.4 (±0.5)	1.1 (±0.2)
$\Delta x_f^{\ddagger}$ (nm)	2.9 (±0.6)	7.7 (±1.5)	1.3 (±0.3)	0.37 (±0.2)
Δx_{eq} (nm)	4.4 (±0.8)	9.9 (±2.6)	3.1 (±0.8)	0.7 (±0.2)
$\Delta x_b^{\ddagger}+\Delta x_f^{\ddagger}$ (nm)	4.4 (±0.8)	10.3 (±2.0)	3.6 (±0.5)	1.5 (±0.3)